Theoretical and Experimental Considerations on the Hammerhead Ribozyme Reactions: Divalent Magnesium Ion Mediated Cleavage of Phosphorus–Oxygen Bonds

Masami Uebayasi,[†] Tadafumi Uchimaru,*[,‡] Tetsuhiko Koguma,[†] Shinya Sawata,[†,§] Takashi Shimayama,[†,⊥] and Kazunari Taira*[,†,∥]

National Institute of Bioscience and Human Technology, National Institute of Materials and Chemical Research, Agency of Industrial Science and Technology, MITI, Tsukuba Science City, 305 Japan, Hitachi Chemical Co., Wadai; Tsukuba 300-42, Japan, and Institute of Materials Science, and Institute of Applied Biochemistry, University of Tsukuba, Tsukuba Science City 305, Japan

Received June 29, 1994[⊗]

Stabilities of oxyphosphoranes were examined with various ionic valences. In general, oxyphosphoranes with more negative charges are less stable. Although dianionic oxyphosphoranes do not have significant lifetimes, at least in the gas phase, a protonation of the dianionic species will enhance its stability. It is of particular interest that the preferred location for protonation of the monoanionic intermediate is found to be in the region between axial and equatorial oxygens despite the fact that most of the negative charges are localized on equatorial oxygens. Placement of the proton between the most negatively charged equatorial oxygens leads to a transition state with a rotation of the P–$O_{equatorial}$(H) bond. Further, we examined the kinetic stability of the dianionic phosphorane neutralized either by two protons or by a divalent magnesium ion. Neutralization by two protons increases the stability of the resulting phosphorane. On the other hand, unexpectedly, the neutral complex between the dianionic phosphorane and the divalent magnesium ion does not have a lifetime. Moreover, the location of the magnesium ion at the frozen configuration of the pentacoordinate intermediate is also found to be in the region between the axial and equatorial oxygens. When all the frozen parameters are completely relaxed, the oxyphosphorane undergoes decomposition by breaking a phosphorus–oxygen bond. These results support the idea that ribozymes are metalloenzymes and magnesium ion itself is capable of cleaving (or forming from the principle of microscopic reversibility) of a phosphorus–oxygen bond by a direct coordination to the translating oxygen. Kinetic data on synthetic ribozymes are in agreement with this interpretation.

More than a decade ago, Cech's group reported that *Tetrahymena* pre-rRNA possesses the catalytic power for the transesterification of phosphodiester bonds and hence, the ability to cleave and/or rejoin nucleotide linkages.[1] Altman's group independently found that the RNA component of RNase P possesses catalytic activity.[2] These discoveries contradicted the long-accepted dogma for enzymes. Before these findings, it was presumed that protein enzymes were the sole catalytic species in biological systems. There are now many examples of RNA molecules which exhibit enzymatic activity and they have come to be known as ribozymes. The list of ribozymes continues to grow. In fact, ribozymes are now considered as the first enzymes that appeared on the earth and thus, are molecular fossils of the "RNA world".[3] Not only are they interesting from this point of view but because of their potential for therapeutic applications, ribozymes have attracted much attention.[4] Extensive experimental work has uncovered the detailed kinetics of ribozyme reactions.[5,6]

There are two mechanistic classes for ribozyme phosphodiester cleavages. In a hammerhead-type ribozyme reaction,[6–9] the cleavage of nucleotide linkages in an RNA molecule takes place via a cyclic oxyphosphorane species (**1**),[10] while an open-chain oxyphosphorane species (**1′**) is involved in the *Tetrahymena* ribozyme reaction.[5] The RNA cleavage intermediate in the former mechanism is the same as the classical mechanism proposed for RNases.[11] Both types of reaction are regarded as a nucleophilic substitution at a tetrahedral phosphate via a pentacoordinate oxyphosphorane intermediate/transition state. Experimental studies using RNA molecules possessing a phosphorothioate at the cleavage site showed that the substitution reaction occurs with inversion of configura-

[†] National Institute of Bioscience and Human Technology.
[‡] National Institute of Materials and Chemical Research.
[§] Institute of Materials Science.
[⊥] Hitachi Chemical Co.
[∥] Institute of Applied Biochemistry.
[⊗] Abstract published in *Advance ACS Abstracts,* November 1, 1994.

(1) Cech, T. R. *Angew. Chem., Int. Ed. Engl.* **1990**, *29*, 759–768.
(2) Altman, S. *Adv. Enzymol.* **1989**, *62*, 1–36.
(3) *The RNA World*; Gesteland, R. F., Atkins, J. F., Eds.; Cold Spring Harbor Laboratory Press: New York, 1993.
(4) *FASEB J. The New Age of RNA*, January issue, **1993**.
(5) (a) Herschlag, D.; Cech, T. R. *Biochemistry* **1990**, *29*, 10159–10171. (b) Young, B.; Herschlag, D.; Cech, T. R. *Cell* **1991**, *67*, 1007–1019. (c) Herschlag, D. *Biochemistry* **1992**, *31*, 1386–1399. (d) Cech T. R. Structure and Mechanism of the Large Catalytic RNAs: Group I and Group II Introns and Ribonuclease P. In *The RNA World*; Gesteland, R. F., Atkins, J. F., Eds.; Cold Spring Harbor Laboratory Press: New York, 1993; pp 239–269.
(6) (a) Fedor, M. J.; Uhlenbeck, O. C. *Biochemistry* **1992**, *31*, 12042–12054. (b) Dahm, S. C.; Derrick, W. B.; Uhlenbeck, O. C. *Biochemistry* **1993**, *32*, 13040–13045.
(7) Symons, R. H. *Trends Biochem. Sci.* **1989**, *14*, 445–450.
(8) Uhlenbeck, O. C. *Nature* **1987**, *328*, 596–600.
(9) Haseloff, J.; Gerlach, W. L. *Nature* **1988**, *334*, 585–591.
(10) Taira, K.; Nishikawa, S. Construction of Several Kinds of Ribozymes: Their Reactivities and Utilities. In *Gene Regulation: Biology and Antisense RNA and DNA*; Erickson, R. P., Izant, J. G., Eds.; Raven Press: New York, 1992; pp 35–54.
(11) Boyer, P. D., Ed. *The Enzymes*, 3rd ed.; Academic Press: New York, 1971; Vol. 4.

0022-3263/94/1959-7414$04.50/0

Chart 1

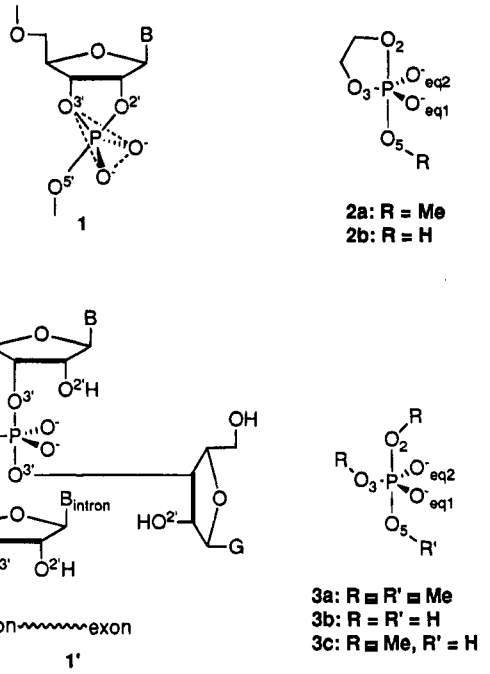

tion at phosphorus.[12–15] The "in-line", $S_N2(P)$ mechanism is thus most likely.

All kinds of ribozyme reactions require divalent metal (i.e., Mg^{2+}) ions as cofactors. For the past few years, we have carried out ab initio investigations on cyclic (**2**) and open-chain (**3**) oxyphosphoranes as models for the intermediate/transition state **1** and **1'** of ribozyme reactions (Chart 1).[16–21] If we consider the fact that two equatorial phosphoryl oxygens are more negatively charged than the other ester oxygens in the transition state, bifurcated metal coordination between the two equatorial phosphoryl oxygens would seem most likely. However, our recent ab initio investigations for open-chain oxyphosphorane **3** suggested that the most preferable Mg^{2+}–oxyphosphorane interactions occur in the regions between equatorial phosphoryl oxygen and the axial oxygen atoms.[16,21] Thus, we suggested the possibility that the *Tetrahymena* ribozyme reaction involves two Mg^{2+} ions in the axial-equatorial regions. In such locations, each Mg^{2+} ion can catalyze the P–O(5′) bond formation and the P–O(3′) bond cleavage; that means ribozymes are metalloenzymes.[16,21] Similar metal chelation was postulated for the Klenow fragment[22] by Steitz's group and they recently proposed a general double-metal ion catalysis mechanism in ribozyme reactions.[23] Recent experimental work by Cech's group indeed revealed that at least one metal ion is involved in the active site of the *Tetrahymena* ribozyme reaction. The magnesium ion was found to be associated with the leaving 3′ axial oxygen atom.[24] This finding is in accord with our proposal that metal ions do not simply act as counter ions.[16,21]

For the hammerhead ribozyme, one metal coordination in the active site has been identified experimentally by Uhlenbeck's group and others: They realized that a substitution of *pro*-R phosphoryl oxygen with sulfur dramatically hinders Mg^{2+}-catalyzed ribozyme reactions and the replacement of Mg^{2+} by Mn^{2+} restores the ribozyme activity on the thio-substrate.[15,25] It has, therefore, been suggested that divalent metal cations directly coordinate to one of the phosphoryl oxygens (*pro-R* oxygen) at the cleavage site.[25–27] In this article, we wish to discuss, from the theoretical standpoint, the hammerhead ribozyme active site and a metal-induced P–O bond cleavage. Kinetic data are in accord with the conclusion based on the calculations.

Experimental Section

Computational Details. Ab initio calculations were carried out using Gaussian 90[28] on an IBM 6000/530 or CRAY X-MP/216. The default procedures were used for geometry optimizations. The five-membered ring opening of ethylene phosphate by nucleophilic attack of methoxide anion is considered as the model, in reverse, of phosphodiester cleavage in hammerhead-type ribozymes.[16–18] We explored the RHF/6-31+G* energy profile for this reaction starting from previously reported RHF stationary points.[17,18] The distances between P and O_2/O_5 were employed as the reaction coordinates. SPARTAN 90[29] provided the three-dimensional representations of the molecular structure and the electrostatic potential.

Kinetic Measurements. Substrates and hammerhead ribozyme used (see Figure 5a for the structures) in this study were chemically synthesized on a DNA synthesizer [380B; Applied Biosystems, Inc. (ABI), CA] as described previously.[30] Kinetic measurements were made at 37 °C, in 50 mM Tris-HCl (pH 6.0–9.0) and 25 mM metal ions. The K_m value for the ribozyme used in 25 mM $MgCl_2$ was 0.02 μM.[30] In order to ensure the condition of $k_{obs} = k_{cat}$, the concentration of substrate was set at above 100 μM. Reactions were monitored by removal of aliquots from the reaction mixture at appropriate intervals and mixing them with an equivalent volume of a solution that contained 100 mM EDTA, 9 M urea, 0.1% xylene cyanol, and 0.1% bromophenol blue. Substrates and 5′-cleaved products were separated by electrophoresis on a 20% polyacrylamide/7 M urea denaturing gel and were detected by autoradiography. The extent of cleavage was determined by quantitation of radioactivity in the bands of substrate and product with a Bio-Image Analyzer (BA100 or BAS2000; Fuji Film, Tokyo).

(12) McSwiggen, J. A.; Cech, T. R. *Science* **1989**, *244*, 679–683.
(13) Rajagopal, J.; Doudna, J. A.; Szostak, J. W. *Science* **1989**, *244*, 692–694.
(14) van Tol, H.; Buzayan, J. M.; Feldstein, P. A.; Eckstein, F.; Bruening, G. *Nucleic Acids Res.* **1990**, *18*, 1971–1975.
(15) Koizumi, M.; Ohtsuka, E. *Biochemistry* **1991**, *30*, 5145–5150.
(16) Uebayasi, M.; Uchimaru, T.; Tanabe, K.; Nishikawa, S.; Taira, K. *Nucleic Acids Res. Symp. Ser.* **1991**, *25*, 107–108.
(17) Storer, J. W.; Uchimaru, T.; Tanabe, K.; Uebayasi, M.; Nishikawa, S.; Taira, K. *J. Am. Chem. Soc.* **1991**, *113*, 5216–5219.
(18) Taira, K.; Uchimaru, T.; Storer, J. W.; Yliniemela, A.; Uebayasi, M.; Tanabe, K. *J. Org. Chem.* **1993**, *58*, 3009–3017.
(19) Uchimaru, T.; Tanabe, K.; Nishikawa, S.; Taira, K. *J. Am. Chem. Soc.* **1991**, *113*, 4351–4353.
(20) Taira, K.; Uchimaru. T.; Tanabe, K.; Uebayasi, M.; Nishikawa, S. *Nucleic Acids Res.* **1991**, *19*, 2747–2753.
(21) Uchimaru, T.; Uebayasi, M.; Tanabe, K.; Taira, K. *FASEB J.* **1993**, *7*, 137–142.
(22) Beese, L. S.; Steitz, T. A. *EMBO J.* **1991**, *10*, 25–33.
(23) Steitz, T. A.; Steitz, J. A. *Proc. Natl. Acad. Sci. U.S.A.* **1993**, *90*, 6498–6502.
(24) Piccirilli, J. A.; Vyle, J. S.; Caruthers, M. H.; Cech, T. R. *Nature* **1993**, *361*, 85–88.
(25) (a) Uhlenbeck, O. C.; Dahm, S. C.; Ruffner, D. E.; Fedor, M. *Nucleic Acids Res. Symp. Ser.* **1989**, *21*, 95–96. (b) Dahm, S. C.; Uhlenbeck, O. C. *Biochemistry* **1991**, *30*, 9464–9469. (c) Slim, G.; Gait, M. J. *Nucleic Acids Res.* **1991**, *19*, 1183–1188.
(26) Yarus, M. *FASEB J.* **1993**, *7*, 31–39.
(27) Pyle, A. M. *Science* **1993**, *261*, 709–714.
(28) Frish, M. J.; Head-Gordon, M.; Trucks, G. W.; Foresman, J. B.; Schlegel, H. B.; Raghavachari, K.; Robb, M. A.; Binkley, J. S.; Gonzalez, C.; Defrees, D. J.; Fox, D. J.; Whiteside, R. A.; Seeger, R.; Melius, C. F.; Baker, J.; Martin, R. L.; Kahn, L. R.; Stewart, J. J. P.; Topiol, S.; Pople, J. A. Gaussian Inc., Pittsburgh, PA, 1990.
(29) Carpenter, J. E.; Hehre, W. J.; Kahn S. D. SPARTAN, version 1.0 Wavefunction Inc., 18401 Von Karmen, #370 Irvine, CA 92715.
(30) Shimayama, T.; Nishikawa, F.; Nishikawa, S.; Taira, K. *Nucleic Acids Res.* **1993**, *21*, 2605–2611.

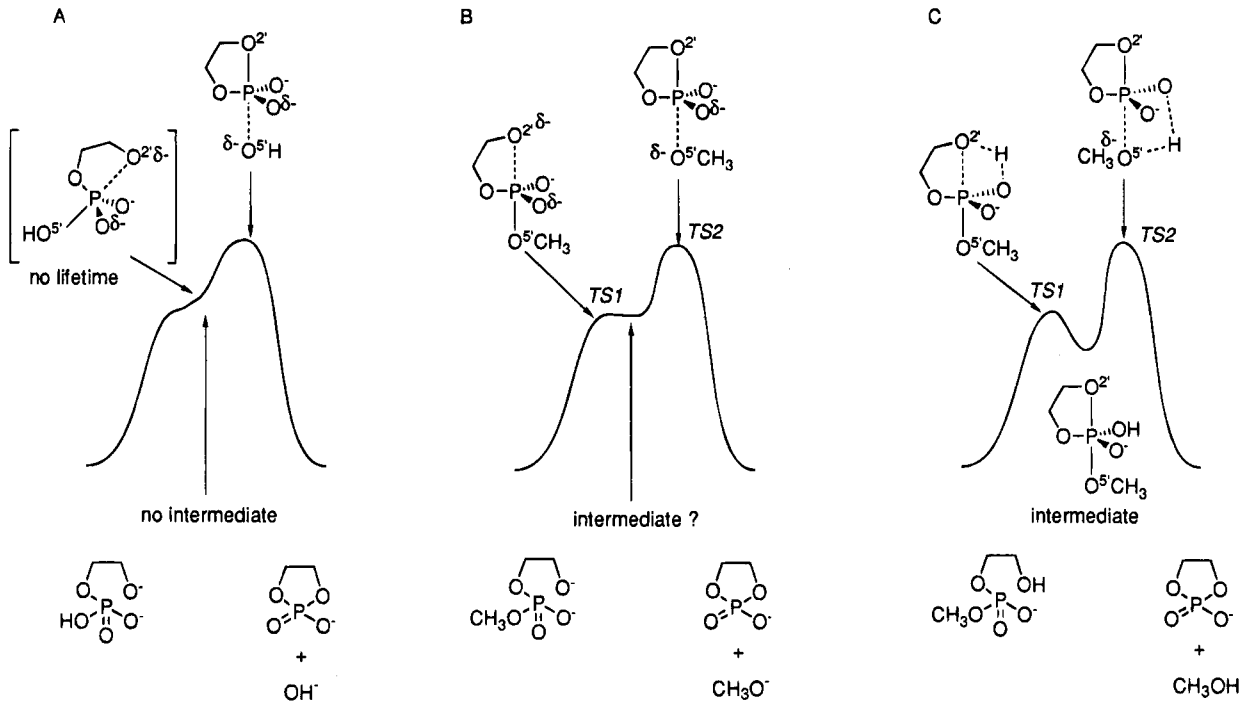

Figure 1. Schematic diagrams of the reaction profile for nulceophilic attack by the O_2 oxygen on phosphorus and the departure of the O_5 oxygen from the cyclic pentacoordinate oxyphosphorane. While Lim and Karplus' dianionic oxyphosphorane **2b** does not exist as an intermediate in the gas-phase (A), monoanionic oxyphosphorane is definitely a stable intermediate (C). The dianionic oxyphosphorane **2a** falls just between these two cases. When the energy profile of dianionic **2a** was calculated at the level of 3-21G*, a very shallow potential energy minimum was found: the lifetime of the intermediate was very short and it was kinetically insignificant.[17,18] The corresponding energy profile of dianionic **2a**, calculated in this study at the level of 6-31+G*, showed no intermediate (B).[41] It is noteworthy that the rate-determining transition-state structures possess $P-O_5$ bond breaking character in all cases.

Results and Discussion

Stability of Oxyphosphoranes. Although a dianionic oxyphosphorane species probably does not exist in the gas-phase,[31,32] our recent ab initio investigations showed that it does exist in the solution phase.[18,33] In the previously reported gas-phase profiles at a lower level (3-21G*) of calculations, a marginally stable dianionic pentacoordinate intermediate **2**, a kinetically insignificant transition state TS1, and the rate-determining overall transition state TS2 were separately found for the ring opening of ethylene phosphate by nucleophilic attack of methoxide anion (Figure 1B).[17,18] However, a single transition state (a single-step mechanism) was observed for the same reaction in the present study at the 6-31+G* level. That is, the dianionic pentacoordinate intermediate could not be located on the 6-31+G* potential surface even after extensive search. Nevertheless, the 6-31+G* profile is in accord with the previous conclusion that the TS2 is the rate-determining transition state: the endocyclic $P-O_2$ bond is much weaker than the exocyclic $P-O_5$ bond. Thus, the single 6-31+G* transition-state structure corresponds to TS2 (with the disappearance of TS1), and it is remarkably asymmetrical regarding the breaking and forming of the $P-O_2$ and $P-O_5$ bonds: the endocyclic $P-O_2$ bond length in the 6-31+G* transition state is 1.673 Å, while the exocyclic $P-O_5$ bond is much longer, 2.275 Å. Accordingly, the imaginary frequency in the single transition state at the 6-31+G* level corresponds to the forming or breaking of the exocyclic $P-O_5$ bond (TS2 transition state) rather than that of the endocyclic $P-O_2$ bond (TS1 transition state).

What we have learned from the series of calculations,[16-21,31-33] regarding the stability of oxyphosphorane intermediates, is that dianionic oxyphosphoranes with small substituents cannot delocalize the negative charges over the entire molecule, thus, they cannot exist in the gas phase (this trend is shown in Figure 1). In other words, larger substituents, waters of hydration, and less negative charge (toward neutralization) tend to stabilize the intermediates (the well-depth for the intermediate becomes deeper). Thus, as mentioned previously, dianionic oxyphosphoranes should have a much longer lifetime once they had been sufficiently solvated.[18,33] It is also emphasized that the structure corresponding to TS2 ($P-O_5$ bond cleavage) is always the rate-determining transition state structure.

From these observations, it is expected that, once dianionic oxyphosphoranes are complexed with divalent metal ions such as Mg^{2+} ions (similar to Figure 1C), the resulting neutral oxyphosphorane-complexes are stable. However, this was not the case and the detailed results will be presented in the Preferred Coordination Sites for Mg^{2+} Ions and Mg^{2+}-Mediated Cleavage of Phosphorus–Oxygen Bonds section.

Preferred Coordination Sites for Proton. We examined the preferred protonation site on the dianionic oxyphosphorane **2a**. The energy profile of the resulting monoanionic oxyphosphorane **2a** of different conformation is shown in Figure 2. The energy is given for the calculations at 3-21G* level. However, when several stationary points were re-checked at different basis set

(31) Lim, C.; Karplus, M. *J. Am. Chem. Soc.* **1990**, *112*, 5872–5873.
(32) Dejaegere, A.; Lim, C.; Karplus, M. *J. Am. Chem. Soc.* **1991**, *113*, 4353–4355.
(33) Yliniemela, A.; Uchimaru, T.; Tanabe, K.; Taira, K. *J. Am. Chem. Soc.* **1993**, *115*, 3032–3033.

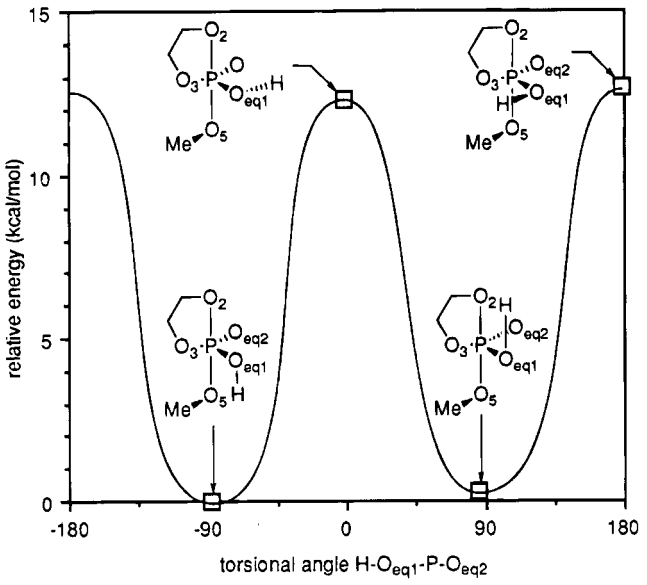

Figure 2. RHF/3-21-G* energy profile for the rotation of the equatorial P–O_{eq1}(H) bond. The energies are plotted as a function of the torsional angle about $HO_{eq1}PO_{eq2}$. The stationary points were fully optimized. The energy profile shows a double well shape whose minima are almost the same in energy (the difference is 0.3 kcal/mol). The rotational transition states are 12.7 (τ = 178.5°) and 12.3 (τ = −0.9°) kcal/mol higher in energy as compared with the global minimum (τ = −87.8°). The hydrogen on O_{eq1} is located around the equatorial plane in the transition state structures, while the O_{eq1}–H bond is almost parallel to the axial P–O bond for the stable structures. A higher basis set tends to increase the rotational barrier.

levels including 6-31+G*, the overall conclusion was the same. That is, although negative charges were mainly localized on the equatorial oxygens, the proton could not stably locate between these two equatorial oxygens (τ = 0°).[16]

We now explain the features of Figure 2 in more detail. What is the preferred interaction between the dianionic **2a** and a cationic ligand? First, we examined the most stable protonation site for the cyclic **2a**. The singly protonated **2a**, that is overall a monoanion, has the pentacoordinate intermediate with a significant well depth (Figure 1C). The proton on the equatorial oxygen (O_{eq1}) was rotated and the energies were plotted as a function of the torsional angle about τ-H–O_{eq1}–P–O_{eq2} (Figure 2). Considering the fact that the negative charges of the dianionic species locates mostly on the equatorial oxygens, O_{eq1} and O_{eq2}, the bifurcated position (τ = 0°) was expected to be the most favorable protonation site. However, the bifurcated structure was found to correspond to the rotational transition state. The rotational profile of Figure 2 indicates two stable conformers in which the proton on the equatorial oxygen O_{eq1} interacts with one of the axial oxygens (O_2 or O_5). The energies of these conformers are almost the same. It can, thus, be concluded that the dianionic cyclic oxyphosphorane **2a** has favorable protonation sites between the equatorial phosphoryl oxygen and the axial oxygens. Also, judging from the optimized structure of monoanionic **2a**, calculated at the 3-21+G* level by Tole and Lim, the preferred protonation site on the dianionic **2a** seems to agree with the results shown in Figure 2.[34] These observations are pertinent to our previous results from studies on the monohydration of **2a**.[17] The equatorially bifurcated hydration of dianionic oxyphosphorane **2a** was found to be less stable than the axial-equatorial hydration.

Preferred Coordination Sites for Cations Can Be Predicted Based on Electrostatic Potentials. The electrostatic potential represents the energy of interaction between a positive charge and a molecule. Thus the electrostatic potential should be useful for interpreting ionic interaction. Previously, we indicated that the locations of metals in proteins and nucleotides can be reproduced by the electrostatic potential of the nearest polar functional groups.[21] Metals were found to be located around the regions where the nearest polar group had the lowest electrostatic potential, although highly ionic metals, such as alkali and heavy alkaline earth metals showed less specific locations.[21]

To examine the most favorable cation-binding site, we calculated the electrostatic potential of **2a**. As shown in Figure 3 (shaded areas), the lowest electrostatic potential of **2a** occurs at the regions above and below the plane containing both the equatorial phosphoryl oxygens and the phosphorus. Thus, bifurcated coordination of cations between equatorial phosphoryl oxygens is not necessarily favorable. These results can explain the rotational energy profile shown in Figure 2.

Preferred Coordination Sites for Mg^{2+} Ions and Mg^{2+}-Mediated Cleavage of Phosphorus–Oxygen Bonds. Mg^{2+}-coordination to dianionic oxyphosphorane **2a** yields a neutral complex. As mentioned in the "Stability of Oxyphosphoranes" section, neutral oxyphosphoranes are, in general, expected to be stable. In fact, neutralization of **2a** by two protons increases the stability of the resulting phosphorane. In pursuit of the preferable Mg^{2+} coordination site, we carried out geometry optimizations for this neutral Mg^{2+}/**2a** complex. At first, the Mg^{2+} ion was placed at the bifurcated position between the equatorial oxygens in the initial structure, so that we would be able to check whether the bifurcated coordination could lead to a transition state, as in the rotational transition state of the proton at τ = 0° (Figure 2), or possibly lead to a potential well. The location of Mg^{2+} ion was optimized with the 3-21G*-optimized frozen structure of oxyphosphorane **2a**. The local minimum was not found around the initial structure. During the optimization routine, the Mg^{2+} ion gradually migrated from the bifurcated position toward the exocyclic oxygen O_5. Hence, the final location of the Mg^{2+} ion was what we expected based on Figures 2 and 3.

Next, full optimization was carried out by placing the Mg^{2+} ion at the bifurcated position between the equatorial oxygens in the initial 3-21G*-optimized structure **2a**. This time, all parameters were relaxed completely and calculations were performed at the 3-21G* level. Once again the Mg^{2+} ion gradually moved toward O_5, during the optimization routine (the same trend was seen from the 6-31+G* calculations). Finally, the axial P–O_5 bond was cleaved to yield ethylene phosphate (Figure 4). No potential-minimum structure was located until the pentacoordinate structure was completely converted into a tetrahedral phosphate. When the initial position of the Mg^{2+} ion was shifted a little bit toward the axial endocyclic oxygen O_2, the cleavage of the P–O_2 bond occurred and the five-membered ring was opened.

These results indicate that, similar to the case of protonation, bifurcated coordination between the equatorial oxygens is not favored for Mg^{2+} ion. Moreover, it is

(34) Tole, P.; Lim, C. *J. Phys. Chem.* **1993**, *97*, 6212–6219.

941087f3

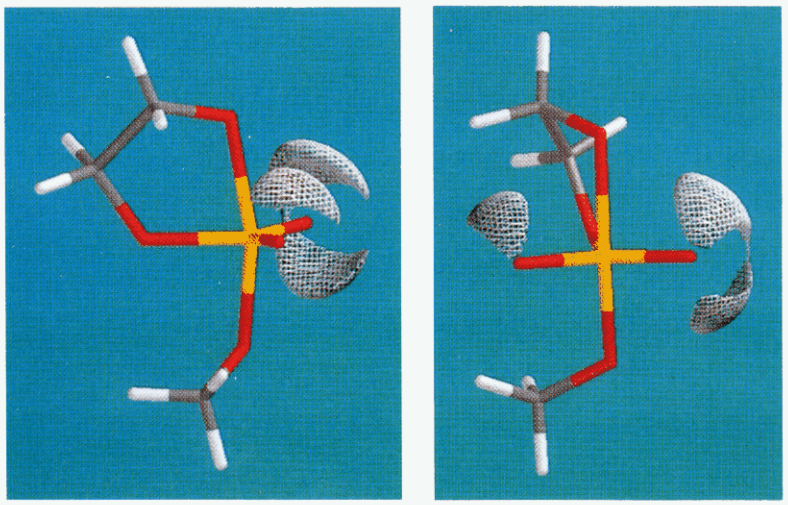

Figure 3. Three-dimensional representations of the surface of the constant electrostatic potential for dianionic oxyphosphorane **2a**. The value of electrostatic potential is −305.0 kcal/mol. The electronic potential was calculated for the 3-21G* optimized geometry by using 3-21G* wave functions.

noteworthy that Mg^{2+} disrupts the pentacoordinate structure, although this complex is totally neutral. In contrast, recall that the well depth of the cyclic dianionic oxyphosphorane intermediate **2a** becomes larger upon protonation. The well depth for singly protonated **2a** (monoanionic **2a**) with respect to the lower transition state TS1 is calculated to be 3.5 kcal/mol at the 3-21G* level,[35] while the corresponding value for dianionic **2a** is 0.24 kcal/mol.[18] Doubly protonated **2a** (neutral **2a**) shows a still larger well depth.[36]

This means that Mg^{2+} ion itself can, because of the microscopic reversibility, catalyze cleavage or formation of phosphorus−oxygen bonds. Hammerhead ribozyme reactions proceed with an inversion of configuration at phosphorus (in-line mechanism via a transition/intermediate structure similar to **2a**) and the Mg^{2+} ion directly coordinates to the *pro-R* equatorial oxygen.[15,25] The potential role of the Mg^{2+} ion was postulated either (i) to neutralize the developing charge in the pentacoordinate transition state/intermediate (by means of a bifurcated structure) or (ii) to facilitate the formation/cleavage of the phosphorus-oxygen bonds (by its potential function as a Lewis acid). Our calculations are in agreement with the latter explanation only. This is in accord with the idea that hammerhead ribozymes are metalloenzymes.[16,21−27]

Mechanism of Action for Hammerhead Ribozymes. In order to elucidate the mechanism of action of hammerhead ribozymes, we have been carrying out kinetic analysis on synthetic ribozymes (Figure 5a).[30,37] A pH−rate profile was measured on the synthetic ribozyme (R32), whose k_{cat} represents the chemical cleavage step.[37] As shown in Figure 5b, the rate-determining chemical-cleavage step can be accelerated by increasing hydroxide ion concentrations. This pH dependency of the ribozyme activity is nearly identical to that reported by Uhlenbeck's group for a hammerhead ribozyme with different binding sequences.[6b] From these observations, one could postulate the involvement of base catalysis, possibly mediated by Mg^{2+}-hydroxide, that abstracts a proton from the 2′-OH of the ribose ring at the cleavage site.[6b] In fact, the experimental data shown by open circles in Figure 5b can be fit with the assumption that a base with a pK_b of 8.5 and limiting k_{cat} value of 21 min^{-1} (the dashed line in Figure 5b) could be involved. However, similar to results reported by Dahm et al.,[6b] a doubling of the substrate concentration in the plateau region increased the k_{cat} value by ~60%, an indication that the plateau originated from a change of the rate-determining step and the pK_b of the base is not 8.5: it is larger than 8.5. This interpretation is in accord with the fact that an apparent deuterium solvent isotope effect decreases upon reaching to the plateau region:[38] The rate-determining step changes from the chemical step to the association step, probably due to deprotonation of uridine and guanosine moieties in a higher pH region.[6b]

The postulated base, Mg^{2+}-hydroxide [POMgOH] with pK_b of 11.4,[39] could indeed abstract a proton from the 2′-OH of the ribose ring to initiate the ribozyme reactions. Alternatively, the active nucleophile (after deprotonation) may be the Mg^{2+}-bound 2′-alkoxide [POMgO(2′)] as shown in Figure 6, because such a positioning of the Mg^{2+} ion could facilitate the cleavage of the phosphorus-oxygen bond (or the formation of the bond from the principle of microscopic reversibility) as discussed in the previous section. We are at present attempting to synthesize a substrate that has a 2′-SH group on the ribose ring at the cleavage site so that the examination of the mechanism shown in Figure 6 becomes feasible. The number of Mg^{2+} ions actually involved in the catalysis still remains obscure. At least one Mg^{2+}-moiety is involved as a base catalyst,[6b] but it is not certain what might act as the acid catalyst to stabilize the leaving 5′-oxygen (TS2 transition state). From the observed thio-effects,[15,25] the *pro-R* oxygen appears to coordinate to one of the Mg^{2+} ions. The first experimental evidence of Mg^{2+} ion acting as an acid catalyst is reported in the case of *Tetrahymena* ribozyme.[24]

The pH−rate profile in the region of pH 6.0 through pH 8.0 in Figure 5b reflects only the concentration of the catalytically competent species such as POMgO(2′) or POMgOH (see the first step of the reaction in Figure 6). Calculations suggest that the second P−O(5′) bond cleav-

(35) Uebayasi, M.; Uchimaru, T.; Taira, K. *Chem. Express* **1992**, *7*, 617−620.
(36) Uebayasi, M.; Uchimaru, T.; Taira, K. Unpublished results.
(37) Sawata, S.; Shimayama, T.; Komiyama, M.; Kumar, P. K. R.; Nishikawa, S.; Taira, K. *Nucleic Acids Res.* **1993**, *21*, 5656−5660.
(38) Sawata, S.; Taira, K. Unpublished results.
(39) Bjerrum, J.; Schwarzenbach, G.; Sillen, L. G. *Stability Constants*; The Chemical Society: London, 1957.

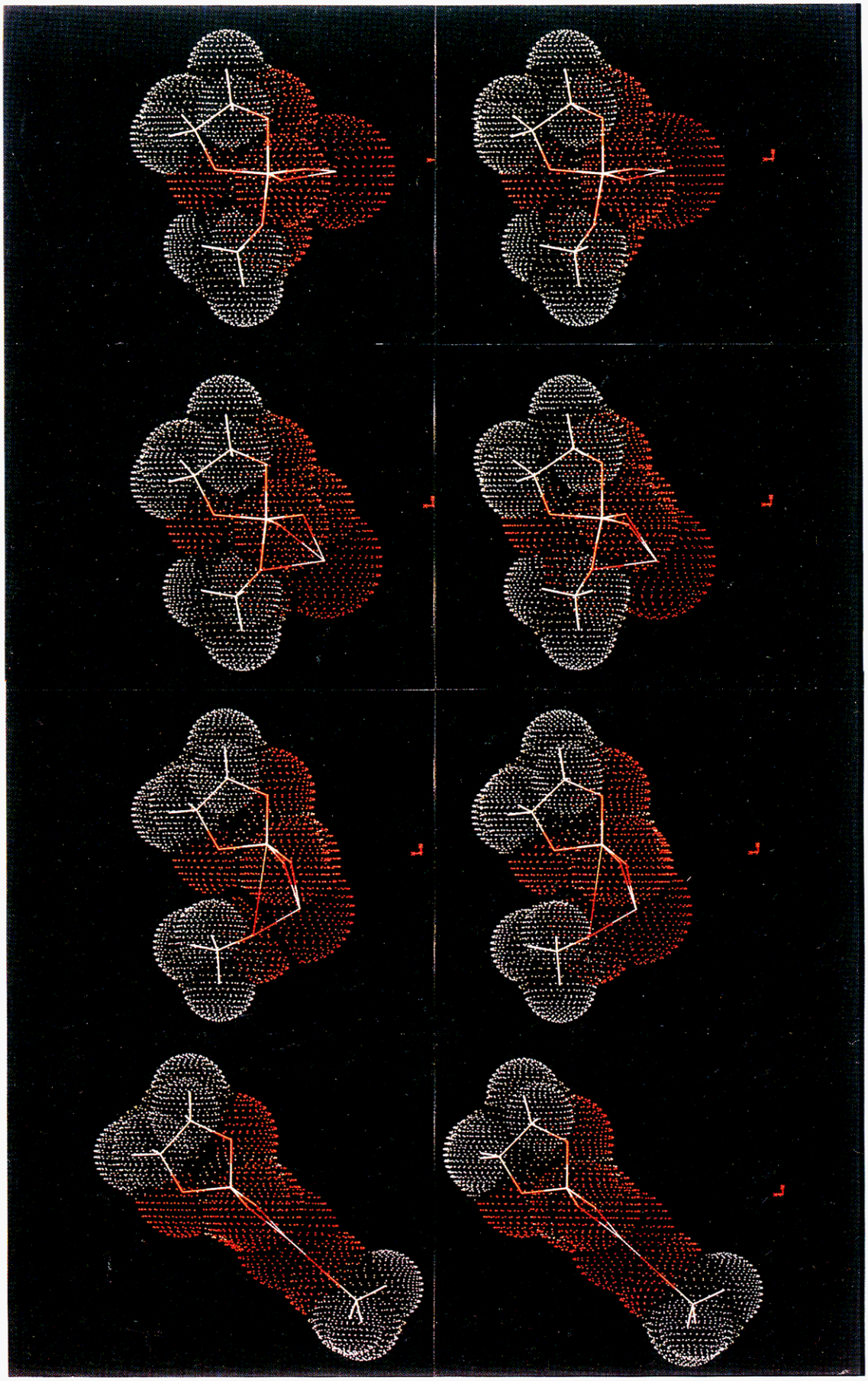

Figure 4. Stereoviews during geometry optimization of the neutral complex between dianionic oxyphosphorane species and Mg^{2+} ion. The Mg^{2+} ion was placed between the equatorial oxygens in the initial structure (top). The Mg^{2+} ion shifted toward the exocyclic oxygen O_5 during the optimization routine (top to bottom). As a result, the full optimization gradually lengthened the $P-O_5$ bond and finally the pentacoordinate oxyphosphorane structure was disrupted to give tetrahedral phosphate (bottom).

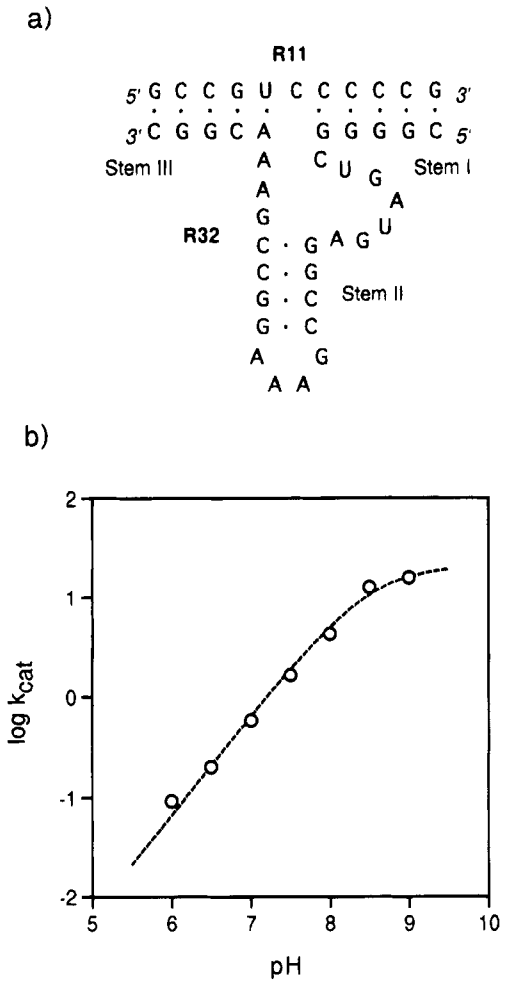

Figure 5. (a) Structures of hammerhead ribozyme (R32) and its substrate (R11). (b) Profile of pH *vs* log(k_{cat}) for hammerhead ribozyme catalyzed reactions. The dashed curve with a slope of unity is a theoretical curve calculated on the assumption of a pK_b of 8.5 and a pH-independent k_{cat} value of 21 min^{-1}. However, an experimental observation that lowering of the apparent isotope effect in higher pH region indicates that the rate-determining step changes from the chemical step to the association step, probably due to deprotonation of uridine moieties, that results in a plateau in the higher pH region.

age step is the overall rate-determining step in the absence of acid catalysis (Figure 1). However, the involvement of acid catalysis in the second step (TS2) was not discernible in the pH-rate profile. Thus, a significant

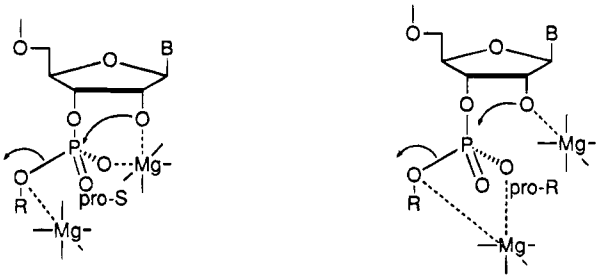

Figure 6. Possible catalytic role of Mg^{2+} ions in the hammerhead ribozyme reactions. Either the Mg^{2+}-hydroxide [POMgOH] with its pK_b value of 11.4 or the Mg^{2+}-bound-2′-alkoxide [POMgO(2′)] as shown in this figure can catalyze the first step of the ribozyme reactions. The second Mg^{2+} ion is capable of acting as a Lewis acid catalyst. At least one Mg^{2+}-moiety directly binds to the *pro-R* oxygen.

energy lowering of the second step (TS2) should have taken place in the hammerhead ribozyme reactions. Since Mg^{2+} ion itself can mediate phosphorus−oxygen bond cleavage and ligation as shown in Figure 4, it is possible that a second Mg^{2+} ion acts as a Lewis acid that directly coordinates to the leaving 5′-oxygen and provides the significant energy lowering of the second step. In fact, our recent finding[40] that solvent isotope effects, after correction of ΔpK_a, were not detected at pH 6.0 during the chemical cleavage step of ribozyme reaction supports the presence of the second Mg^{2+} ion that directly coordinates to the leaving 5′-oxygen and it argues against the involvement of a proton catalysis at the transition state. This conclusion is pertinent to our calculation results and also to the mechanism of double metal ion catalysis proposed by Steitz and Steitz.[23]

In conclusion, our ab initio calculations and kinetic analysis support the idea that Mg^{2+} ion directly coordinates to the leaving 5′-oxygen and facilitates the second step (the overall rate-determining transition state in the absence of catalysis) of the hammerhead ribozyme reaction.

(40) Sawata, S.; Komiyama, M.; Taira, K. *J. Am. Chem. Soc.*, submitted for publication.

(41) RHF/3-21+G* potential energy surface for the open-chain dianionic oxyphosphorane **3a** showed separate transition states for P-O_2 and P-O_5 bond forming/breaking steps and also an oxyphosphorane intermediate with shallow well depth. MP2/6-31+G* calculations for each stationary point suggested nearly identical energy differences between the transition states and the intermediate as compared to the RHF energy gap.[42] Similar results would be expected for the case of the corresponding dianionic cyclic oxyphosphorane **2a**.

(42) Uchimaru, T.; Tsuzuki, S.; Storer, J. W.; Tanabe, K.; Taira, K. *J. Org. Chem.* **1994**, *59*, 1835−1843.